*Nucleic Acids Research, 2005, Vol. 33, No. 21* ***6723–6732***
*doi:10.1093/nar/gki961*

# The effect of osmolytes and small molecule on Quadruplex–WC duplex equilibrium: a fluorescence resonance energy transfer study

**Niti Kumar and Souvik Maiti***

Structural Biology Unit, Institute of Genomics and Integrative Biology, CSIR, Mall Road, New Delhi 110 007, India

Received August 8, 2005; Revised and Accepted October 29, 2005

## ABSTRACT

**The structural competition between the G-quadruplex and Watson–Crick duplex has been implicated for the repetitive DNA sequences, but the factors influencing this competitive equilibrium in the natural and pharmacological context need to be elucidated. Using a 21mer 5′-Fluorescein-d[$(G_3TTA)_3G_3$]-TAMRA-3′ as a model system, extensive fluorescence resonance energy transfer analysis was carried out to investigate sensitivity of this equilibrium to osmotic stress and quadruplex selective small molecule. The binding affinities and kinetics involved in the hybridization of quadruplex to its complementary strand in the absence and presence of different concentrations of osmolytes (ethylene glycol and glycerol) and a quadruplex selective ligand (cationic porphyrin-TMPyP4) were determined. The presence of osmolytes and cationic porphyrin decreased the binding affinity of quadruplex to its complementary strand and slowed the kinetics of the reaction by delaying the hybridization process. Our binding data analysis indicates that the presence of either osmolytes or porphyrin increase the amount of quadruplex in the equilibrium. In 100 mM KCl solution, when 30 nM of each of the components, i.e. quadruplex and the complementary strand, were mixed together, the amount of quadruplex present in the system under equilibrium were 17.6, 23.4, 23.1 and 19.6 nM in the absence and presence of 10% ethylene glycol, 10% glycerol and 150 nM TMPyP4, respectively. Fluorescence melting profile of quadruplex in the absence and presence of these perturbants confirm the findings that osmolytes and cationic porphyrin stabilize quadruplex, and thus, shift the equilibrium to quadruplex formation.**

## INTRODUCTION

Guanine-rich oligonucleotides have the potential to form unusual secondary structures comprising of four Hoogsteen-paired coplanar guanines (1). The level of interest in these structures has increased markedly since the past decade as the evidence for their possible functional roles *in vivo* has accumulated. These guanine-rich segments are found in biologically significant regions of the genome, such as telomeres (2), immunoglobulin switch regions (3), gene promoter regions (4,5) and sequences associated with human diseases (6). Several proteins that bind to G-quadruplexes have been identified (7–12) and some of these proteins promote the formation of quadruplex structures (8,9,13). Many small molecules specifically bind to quadruplexes, and act as selective inhibitors of telomerase, a potential target for anticancer therapy (14,15). The first draft of the human genome has provided additional impetus for exploring the role of unusual DNA structures in general and quadruplexes in particular (16–18).

Inside the cell, G-rich sequences are present along with their complementary C-rich strands. Therefore, such multi-stranded DNA secondary structures compete with the normal Watson–Crick (WC) duplexes formed by the interaction with the complementary strands. Quadruplex and WC duplex exist in an environmentally (natural or artificial) controlled dynamic equilibrium, transient shifts in equilibrium favor either quadruplex or duplex formation, as required for the execution of biological function. Duplex–Quadruplex interconversions have been studied for different sequences (19–30). Using an equimolar mixture of the telomeric oligonucleotides d[$AGGG(TTAGGG)_3$] and d[$TCCC(AATCCC)_3$], Phan and Mergny (25) showed that at physiological pH, temperature and salt concentration, telomeric DNA was predominantly in the duplex form. However, at higher salt concentration or lower pH, the G-quadruplex and/or the I-motif efficiently compete with the WC duplex. In another study (29), it was shown that the Tetrahymena telomere sequences d[$G_4(T_2G_4)_3$], d[$G_3(T_2G_3)_3$] and sequences related to regions of the *c-myc* promoter

*To whom correspondence should be addressed. Tel: +91 11 2766 6156; Fax: +91 11 2766 7471; Email: souvik@igib.res.in

$d(G_4AG_4T)_2$, $d(G_4AG_3T)_2$ preferentially adopt quadruplex structure in potassium-containing buffers, and retain this structure even in the presence of a 50-fold excess of their complementary C-rich strands, but the duplex form predominates in the presence of sodium. Li *et al*. (30) investigated competitive structural transition among the G-rich quadruplex, C-rich i-motif, and the corresponding WC duplex for $dG_3(T_2AG_3)$, $d(C_3TA_2)_3C_3$ and $dG_3(T_2AG_3)_3/d(C_3TA_2)_3C_3$ using ITC, DSC, PAGE, CD, UV and stopped-flow kinetic techniques. ITC and PAGE experiments confirmed WC duplex formation upon addition of the complementary strand. The binding constant of the two DNA strands in the presence of 10 mM $Mg^{2+}$, pH 7 was 400 times larger than that in the presence of 100 mM $Na^+$, pH 5.5. Kinetic studies showed that the dissociation of the single-stranded structured DNAs is the rate-limiting step for the WC duplex formation. Recently, Green *et al*. (27) reported the kinetics of opening of the DNA quadruplex formed by the human telomeric sequence with a peptide nucleic acid (PNA) trap. This opening was zero order with respect to PNA, also indicating that the initial step is a rate-limiting internal rearrangement of the quadruplex.

The Quadruplex–WC equilibrium is under the subtle influence of many factors, which involves the contribution from cellular environment, such as pH, cations and temperature. However, this dynamic equilibrium can also be influenced by molecular crowding as a living cell is inherently crowded with various biomolecules. Molecular crowding agents such as osmolytes substantially affect the rate of reactions, and thus, their influence on G-rich and C-rich secondary structures is critical for revealing the *in vivo* scenario and the on-set mechanism of diseases related to these DNA structures. Miyoshi *et al*. (31) have demonstrated that molecular crowding prevents duplex formation between G-rich and C-rich DNA, and this further indicates that structural polymorphism in DNA structures is induced by molecular crowding, *in vivo*. These multi-stranded G-rich structures also serve as attractive targets in the pharmacological context. Cationic porphyrins are known to bind and stabilize different types of quadruplexes and 5,10,15,20-tetrakis-(1-methyl-4pyridyl)-21H,23H-porphine (TMPyP4) is an effective telomerase inhibitor with an $EC_{50}$ of 6.5 μM (14) in a cell-free assay. TMPyP4 also binds to the intramolecularly folded parallel G-quadruplex present in the *c-myc* promoter and most likely converts it to a mixed parallel/antiparallel G-quadruplex suppressing *c-myc* transcriptional activation (32,33). Similar transitional changes were also observed for telomeric sequences from *Oxytricha* species (34,35). For the achievement of therapeutic selectivity by targeting G-quadruplexes, it is necessary to understand the mechanism of this Quadruplex–WC duplex equilibrium in the intracellular milieu and in the presence of G-interactive foreign ligands.

To examine the effect of different environmental perturbations on the quadruplex to duplex transition, we studied the binding and kinetics behavior of a preformed G-quadruplex in the presence of its complementary C-rich strand by fluorescence resonance energy transfer (FRET) in 50 mM MES buffer, pH 7 with 100 mM KCl. FRET has been successfully applied to characterize quadruplex and I-motif formation from G-rich and C-rich sequences, respectively (36–38). The quadruplex formed by $d(G_3TTA)_3G_3$ is stabilized by three G-quartets and three TTA loops. We used FRET to assess the binding affinity of this oligonucleotide to metal ion ($K^+$), leading to the formation of quadruplex. The thermodynamic stability of quadruplex was determined in the presence and absence of osmolytes (ethylene glycol and glycerol), and quadruplex selective small ligand TMPyP4, followed by the estimation of the binding affinity and kinetics of opening of the preformed quadruplex upon the addition of its 21mer complementary C-rich strand $d[C_3(TAAC_3)_3]$ in the above mentioned conditions.

## MATERIALS AND METHODS

The 21mer oligonucleotide d(GGG TTA GGG TTA GGG TTA GGG) unlabeled and labeled with 5′-Fluorescein and 3′-tetramethylrhodamine (TAMRA) and its corresponding complementary strand d(CCC TAA CCC TAA CCC TAA CCC) (all HPLC purified) were obtained from Sigma Genosys. The concentration of unlabeled oligonucleotide solutions was determined from absorbance at 260 nm and 80°C, using a molar extinction coefficient of 215 $mM^{-1}$ $cm^{-1}$ for G-rich and 171 $mM^{-1}$ $cm^{-1}$ for C-rich strands. These values were calculated by extrapolation of the tabulated values of the dimers and monomer bases (39) at 25°C to high temperatures using procedures reported earlier (40). Concentration of the labeled oligonucleotide was determined by measuring the absorbance of the attached Fluorescein moiety at 496 nm using a molar extinction coefficient of $4.1 \times 10^4$ $M^{-1}$ $cm^{-1}$ (36). Osmolyte concentrations of 5%, 10% (wt/vol) of ethylene glycol and glycerol from Aldrich were prepared. G-quadruplex interactive drug, TMPyP4 (5,10,15,20-tetrakis-(1-methyl-4pyridyl)-21H, 23H-porphine) was obtained from Sigma. Its concentration was determined from absorbance at 424 nm using a molar extinction coefficient of $2.26 \times 10^5$ $M^{-1}$ $cm^{-1}$. All other reagents were of analytical grade. Milli Q water was used in all the experiments. All experiments except for $K^+$ binding affinity measurement were carried out in 50 mM MES buffer, pH 7 with 100 mM KCl. CD spectra were measured by a Jasco spectropolarimeter (model 715, Japan), equipped with a thermoelectrically controlled cell holder, and a cuvette with a path length of 1 cm. CD spectrum for quadruplex (5 μM) in the absence and presence of osmolyte, and with equimolar concentration of complementary strand was recorded between 220 and 325 nm at 15°C in 50 mM MES buffer, pH 7 with 100 mM KCl. UV melting of unlabeled $d(G_3TTA)_3G_3$ (2 μM) in 100 mM KCl buffer, pH 7 was carried out by PerkinElmer Lambda 35 spectrophotometer, equipped with a thermoregulated Peltier element. Absorbance at 295 nm was recorded as a function of temperature with heating and cooling rate of 0.2°C/min.

### Steady state experiments

Fluorescence experiments were carried out using Fluoromax 4 (spex) spectrofluorimeter and FLUOstar OPTIMA from BMG labtech (Germany). In Fluoromax 4 (Spex) spectrofluorimeter, excitation wavelength was set at 480 nm (though the absorption maximum of donor is at 492 nm) to minimize acceptor absorption, and the emission spectra were recorded from 500 to 700 nm. To construct the melting profile of the quadruplex-$K^+$ (30 nM) with a heating rate of 0.3°C/min, donor (Fluorescein) emission at 520 nm, defined as $I = (F - F_0)/$

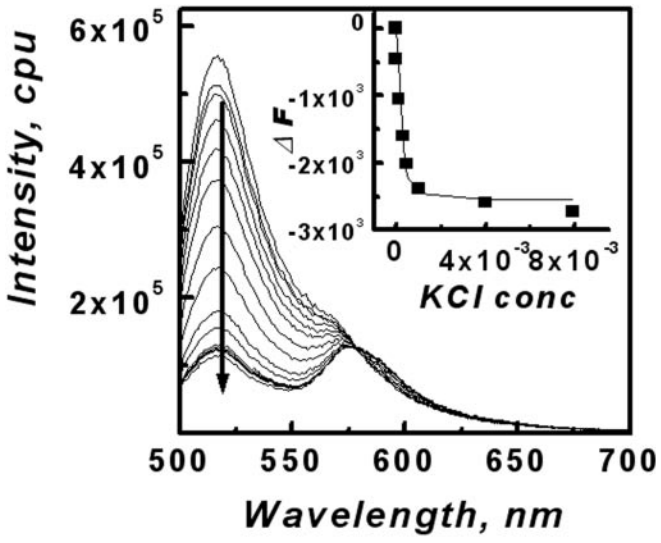


**Figure 1.** Fluorescence emission spectra of the dual labeled d[$(G_3TTA)_3G_3$] (12 nM) at 10°C in 50 mM MES buffer, pH 7 at different KCl concentration. Arrow headed line indicates the KCl increment direction. Inset shows fluorescence emission intensity at 520 nm ($\Delta F$ as described in the text) of the dual labeled d[$(G_3TTA)_3G_3$] versus KCl concentration.

($F_{max} - F_0$), was plotted as a function of temperature, where $F$ is the fluorescence at any temperature and $F_0$ and $F_{max}$ are lowest and highest fluorescence observed. The melting profile of quadruplex-$K^+$ (30 nM) was also analyzed in the presence of 10% (wt/vol) ethylene glycol, 10% (wt/vol) glycerol, and 150 nM of quadruplex selective small molecule TMPyP4.

To determine the $K^+$ binding affinity of G-rich strand, fluorescence experiments were carried out at 20°C using fixed concentration (12 nM) of dual labeled G-rich strand and varying KCl concentration (0–10 mM). Similar binding study was performed for quadruplex-$K^+$ strand (12 nM) and varying its complementary C-rich strand (0–100 nM) at 20°C in 50 mM MES buffer, pH 7 with 100 mM KCl.

To obtain the binding affinity of the oligonucleotide for metal ions at a particular temperature, $\Delta F = F - F_0$ (where $F_0$ and $F$ is the initial and subsequent fluorescence intensities of the donor-fluorescein, at 520 nm upon KCl addition) was plotted against the metal ion concentration, shown in the inset of Figure 1. Two metal ions can bind to one oligonucleotide, so the following fitting equation was used,

$$\Delta F = (\Delta F_\infty [M^+]_0^2 K_M)/(1+[M^+]_0^2 K_M) \quad \mathbf{1}$$

where $K_M$ is the binding constant, $[M^+]_0$ is the initial concentration of $K^+$ ions and $\Delta F_\infty = F_\infty - F_0$ [the subscripts $\infty$ and 0, defines the bound (quadruplex) and free (extended) form].

FLUOstar OPTIMA fluorescence plate reader was used to determine the binding affinity of G-quadruplex to its complementary strand in the presence of osmolytes and G-interactive small molecule. The plate reader provides the advantage of working with many samples, at very dilute concentrations, and on systems that suffer from thermodynamic and kinetic inertia, requiring prolonged incubation. The experiments were done in 384 well plates, using excitation (480 nm) and emission (520 nm) filters for fluorescein. The wells were loaded with the solution of fixed concentration of preformed quadruplex (12 nM) and increasing concentrations of complementary strand (0–100 nM). Sample mixtures were incubated for a period of 12 h at 20°C, to ensure that equilibrium was attained and the plate was read at 520 nm. Similar experiments were carried out in 50 mM MES buffer, pH 7 with 100 mM KCl containing different concentrations of osmolytes [0, 5, 10% (wt/vol) ethylene glycol and glycerol] and different concentrations of TMPyP4 (60 and 120 nM). For analysis of data, the observed fluorescence intensity was considered as the sum of the weighted contributions from folded G-quadruplex strand and extended G-strand:

$$F = F_0(C_t - C_b) + F_b C_b \quad \mathbf{2}$$

where $F$ is the observed fluorescence intensity at each titrant concentration, $F_0$ and $F_b$ are the respective fluorescence intensities of initial and final states of titration, and $C_t$ and $C_b$ are the concentrations of total and unfolded G-strand, respectively. Assuming 1:1 stoichiometry for the interaction in case of complementary strand binding, it can be shown that:

$$C_b^2 - C_b([Q]_0 + [C]_0 + 1/K_A) + [Q]_0[C]_0 = 0 \quad \mathbf{3}$$

where $K_A$ is the association constant, $[Q]_0$ is the total G-strand concentration, and $[C]_0$ is the total complementary strand concentration.

From Equations 2 and 3, it can be shown that:

$$\Delta F = (\Delta F_{max}/2C_0)\{[Q]_0 + [C]_0 + 1/K_A\} - \sqrt{([Q]_0 + [C]_0 + 1/K_A)^2 - 4[Q]_0[C]_0} \quad \mathbf{4}$$

Where $\Delta F = F - F_0$ and $\Delta F_{max} = F_{max} - F_0$.

### Kinetic experiments

A detailed insight into the unfolding kinetics of quadruplex requires approximation of the unfolding rate constants. The opening up of quadruplex (30 nM) upon addition of equivalent concentration of the complementary strand was monitored as the increase in fluorescence intensity at 520 nm with respect to time, using instead of monitored, as the increase in fluorescence intensity at 520 nm as a function of time using Fluoromax 4 (spex) spectrofluorimeter. The kinetics experiments were conducted in the presence of various concentrations of osmolytes [0, 5, 10% wt/vol ethylene glycol and glycerol] and in the presence of 150 nM TMPyP4 in MES buffer, pH 7 with 100 mM KCl. Double exponential decay fitting was carried out according to the equation:

$$\Delta F = A_1 e^{-t/\Gamma_1} + A_2 e^{-t/\Gamma_2} + A_3 \quad \mathbf{5}$$

Where $\Gamma_1$ and $\Gamma_2$ are the time constants of the decay and $A_1$ and $A_2$ are their respective amplitudes. $A_3$ is the fluorescence intensity at $t = \infty$. The observed rate constant was calculated from the mean time constant ($\Gamma$), $k = [1/\Gamma]$, where ($\Gamma$) was calculated as,

$$(\Gamma) = (A_1\Gamma_1 + A_2\Gamma_2)/(A_1 + A_2). \quad \mathbf{6}$$

## RESULTS

### FRET: a tool for competition study

Inside the cell most G-rich sequences with the potential to adopt G-quadruplexes are present along with their

complementary C-rich strand, which generates competing duplex structures depending on the cellular conditions. FRET can be used to probe the secondary structure formed by a guanosine-rich DNA fragment with fluorescein (donor) and TAMRA (acceptor) at 5′ and 3′ ends of the oligonucleotide, respectively. In this study, we report the use of FRET as a tool in the competition study between quadruplex and duplex transition. The formation of the quadruplex from a G-rich oligonucleotide, in the presence of monovalent cations, is accompanied by the decrease in the distance between the donor and the acceptor molecule leading to a greater energy transfer from the donor to the acceptor. Upon hybridization to its complementary C-rich sequence, the donor and acceptor are separated by a larger distance, resulting in lesser energy transfer and higher fluorescence intensity in the donor region. Figure 1 shows a representative plot for FRET change for the dual labeled d(GGG TTA GGG TTA GGG TTA GGG) in 50mM MES buffer, pH 7.0, upon increasing the concentration of $K^+$ (0–10 mM), leading to a decrease in fluorescence intensity of fluorescein at 520 nm. A clear isoemissive point obtained at 575 nm indicates that there are only two states: extended (random coil) and folded (quadruplex) forms in the aqueous salt solution and that the presence of the metal ions shifts the equilibrium toward the quadruplex form. Using Equation 1, the binding affinity of $K^+$ at 20°C was determined to be 2.5 (±0.3) × $10^7$ $M^{-2}$, which is in agreement with the literature value (41).

The melting profile of the quadruplex (30 nM) was characterized in the presence of 100 mM KCl by monitoring the change in fluorescence of the labeled oligonucleotide with increasing temperature. Figure 2 shows a representative graph of fluorescence spectra at different temperatures. The plot of fluorescence intensity at 520 nm versus temperature (inset Figure 2) exhibits a sigmoid curve, the inflection point gave the $T_m$ value of 60.5 (±1)°C, which correlates with the literature findings. Furthermore, the independence of $T_m$ over a wide concentration range (10 nM–1 μM, data not shown) of dual labeled 5′-Fluorescein-d[$(G_3TTA)_3G_3$]-TAMRA-3′ indicates intramolecular folding for the given quadruplex sequence. The thermodynamic parameters for quadruplex melting were estimated using the procedure described by Bonnet *et al*. (42). The dissociation constant of the quadruplex ($K_d$) was determined using the following equation:

$$K_d = [(F - F_c)/(F_o - F)] \quad \mathbf{7}$$

where $F$ is the observed fluorescence intensity at a given temperature and $F_c$ and $F_o$ are the fluorescence intensities of the quadruplex in the closed and open forms, respectively. The values of $F_c$ and $F_o$ were measured at lowest and highest temperatures, respectively in the melting curve. Using the relation $\Delta G = -RT \ln K_d = \Delta H - T\Delta S$; $\Delta H$ was determined from the slope of plot of $R\ln\{(F_o - F)/(F - F_c)\}$ versus $1/T$, where $R$ represents the gas constant and $T$ is the absolute temperature (K). The $\Delta H$ obtained for quadruplex melting in 100 mM KCl was found to be 39.8 (±2) kcal/mol and $\Delta S$ was found to be 122.4 (±6) cal/mol/K.

Next, we analyzed the effect of increasing complementary strand concentration (0 to 100 nM) on quadruplex to duplex transition in 100 mM KCl buffer. Figure 3 shows the fluorescence spectra of the quadruplex-$K^+$ (12 nM) upon successive addition of its C-rich complementary strand, d(CCC TAA CCC TAA CCC TAA CCC). We observed that unfolding of intramolecular quadruplex and its subsequent hybridization to the complementary strand is an extremely slow process, and thus, requires prolong incubation to achieve the equilibrium (shown below). To overcome such a kinetic barrier, we allowed 3–4 h incubation to obtain a stable florescence reading. As shown in Figure 3, the fluorescence intensity of fluorescein increases with increase in complementary strand concentration and an isoemissive point at 575 nm was obtained. This explains that addition of the complementary

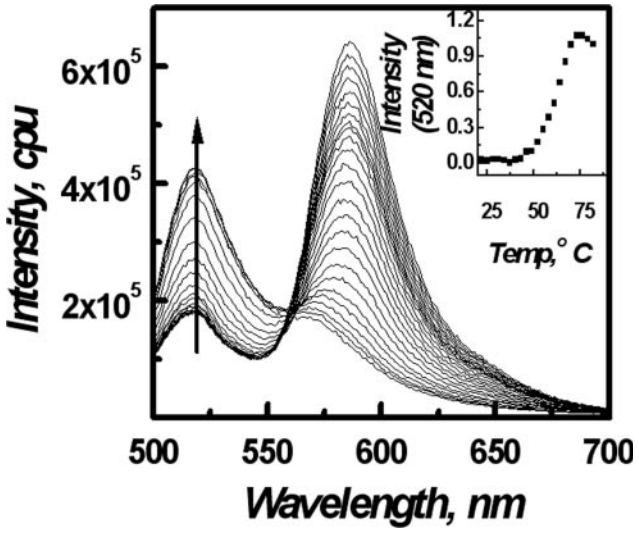


**Figure 2.** Fluorescence emission spectra of the dual labeled d[$(G_3TTA)_3G_3$] (30 nM) in 50 mM MES buffer with 100 mM KCl, pH7 at different temperatures. Arrow headed line indicates the temperature increment direction from 20 to 90°C. Inset shows intensity at 520 nm versus temperature plot.

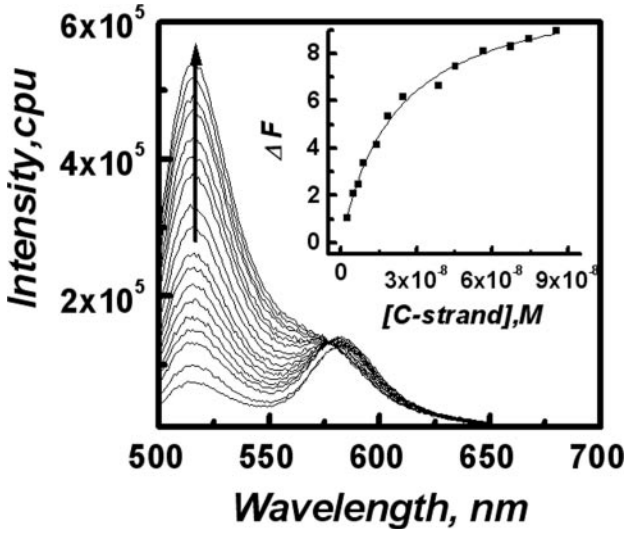


**Figure 3.** Fluorescence emission spectra of the dual labeled quadruplex-$K^+$ complex (12 nM) in 50 mM MES buffer with 100 mM KCl, pH7 at different complementary strand concentration. Arrow headed line indicates complementary strand concentration increment. Inset shows the plots of relative fluorescence emission intensity at 520 nm ($\Delta F$ as described in the text) versus complementary strand concentration in KCl buffer at 20°C.

strand leads to the unfolding of intramolecular quadruplex and subsequent hybridization to G-rich strand to form duplex. The plot of ratio of intensity of fluorescein versus complementary strand concentration is shown in inset of Figure 3. The binding affinity to the complementary strand at 20°C calculated from this plot, using Equation 4, was found to be 4.1 (±0.15) $\times 10^7$ $M^{-1}$ in the presence of $K^+$ ions.

To investigate the binding kinetics of the above system in 100 mM KCl, precise estimation of quadruplex unfolding rate constant upon hybridization to its complementary strand was required. We observed that in the presence of $K^+$ ions, the rate of opening was relatively slow but could be followed by conventional spectrophotometer at 20°C as shown in Figure 4a. Analysis of the kinetic data showed that the kinetics is second order in nature and the obtained rate constant was 10.7 (±0.3) $\times 10^{-5}$ $M^{-1}$ $s^{-1}$ at 20°C in 100 mM KCl solution.

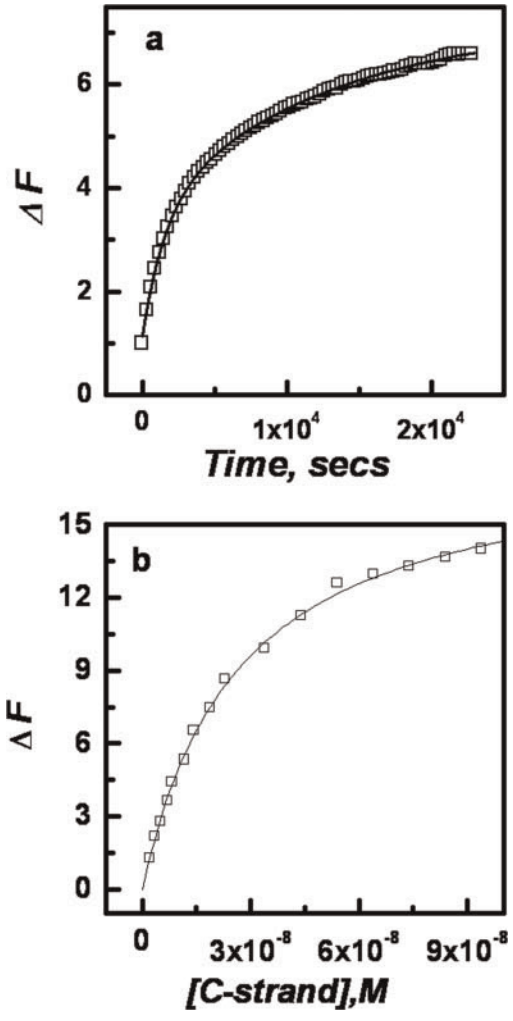


**Figure 4.** (**a**) Opening up of the quadruplex-$K^+$ (30 nM) at 20°C upon addition of equimolar concentration of C-strand measured in 50 mM MES buffer, pH 7 containing 100 mM KCl; (**b**) Plots of relative fluorescence emission intensity ($\Delta F$ as described in the text) of quadruplex-$K^+$ (12 nM) at 520 nm measured using FLUOstar OPTIMA plate reader versus complementary strand concentration in KCl buffer, pH 7 at 20°C.

As the kinetics was very slow, to make the experiments high throughput without disturbing equilibrium, the binding affinity of the quadruplex to its respective complementary strand was estimated using FLUOstar OPTIMA plate reader, which provides the advantage to work on many systems that suffer from thermodynamic and kinetic inertia, requiring prolonged incubation simultaneously. Owing to the slow kinetics of the reaction, and to ensure attainment of equilibrium, the samples were given incubation of 12 h at 20°C and the intensity was recorded at 520 nm. The binding affinity obtained by this method was 3.86 (±0.2) $\times 10^7$ $M^{-1}$ (Figure 4b), which approximated well with the value obtained from Fluoromax 4 (spex) spectrofluorimeter based study. FLUOstar OPTIMA plate reader can thus, be reliably used to determine the binding affinity.

### Role of molecular crowding on competition

Biochemical studies are regularly conducted in highly dilute solutions, whereas the intracellular milieu is extremely crowded (43). To analyze the effect of osmolytes as crowding agents on the stability of G-rich secondary structures, the melting of quadruplex was performed in the presence of 10% (wt/vol) ethylene glycol and 10% (wt/vol) glycerol in 100 mM KCl solution. The plot of fluorescence intensity at 520 nm versus temperature displayed a sigmoid curve in each case (Supplementary Figure S3). The inflection point of the melting curve yielded the $T_m$ value as 66.2 (±1)°C in the presence of ethylene glycol and 65.7 (±2)°C in the presence of 10% glycerol. The observed increment in $T_m$ was found out to be 5.2 and 5.7°C in the presence of 10% ethylene glycol and glycerol, respectively. Further analysis of the melting curves, as explained above, gave corresponding $\Delta H$ value as 45.7 (±2.0) Kcal/mol in the presence of ethylene glycol and 49.4 (±1.5) Kcal/mol in the presence of glycerol, as compared to a value of 39.8 (±2) Kcal/mol in the absence of osmolyte. The entropy contribution ($\Delta S$) for the melting was estimated to be 134.9 (±3) cal/mol/K and 145.9 (±4) cal/mol/K for 10% ethylene glycol and 10% glycerol, respectively, compared to 122.4 (±6) cal/mol/K in the absence of osmolytes.

Furthermore, to investigate the effect of osmolytes on quadruplex to duplex transition in 100 mM KCl buffer, the binding affinity of quadruplex to its complementary strand was determined in the presence of different concentrations (0, 5 and 10%) of osmolytes. Figure 5 shows the change in fluorescein intensity versus complementary strand concentration in the absence and presence of 5% (wt/vol) and 10% (wt/vol) ethylene glycol and glycerol, respectively. The binding affinities obtained were 2.4 (±0.15) $\times 10^7$ $M^{-1}$ and 1.2 (±0.21) $\times 10^7$ $M^{-1}$ in the presence of 5 and 10% (wt/vol) ethylene glycol, respectively, whereas corresponding values in the presence of 5 and 10% (wt/vol) glycerol were 2.6 (±0.1) $\times 10^7$ $M^{-1}$ and 1.3 (±0.2) $\times 10^7$ $M^{-1}$, respectively, against the value of 3.86 (±0.2) $\times 10^7$ $M^{-1}$ obtained in the absence of osmolytes. The data reveals that the binding affinity of quadruplex towards the complementary strand reduces in the presence of osmolytes.

Next, we elucidated the kinetics of quadruplex (30 nM) opening in the absence and presence of osmolytes (5 and 10% wt/vol), upon the addition of equimolar complementary strand. Figure 6 shows a representative plot of kinetic study,

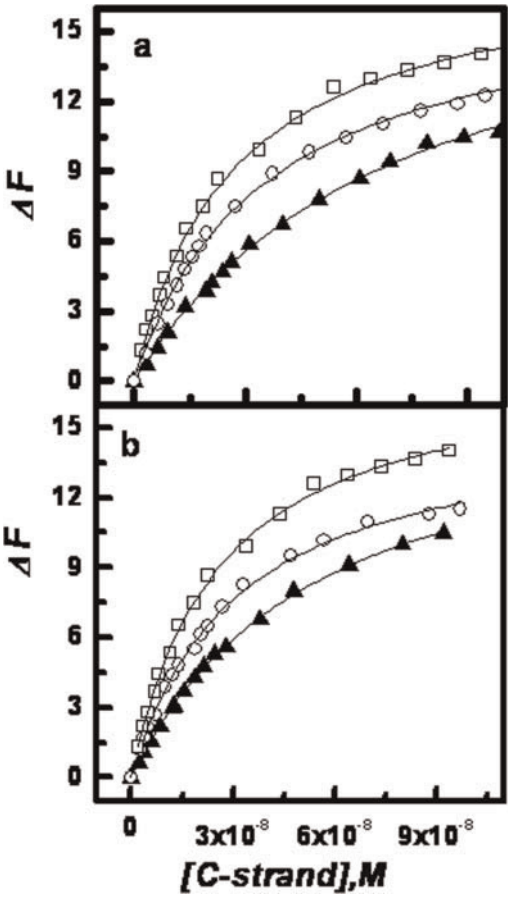


**Figure 5.** (a) Plots of relative fluorescence emission intensity of Quadruplex-$K^+$ (12 nM) at 520 nm ($\Delta F$ as described in the text) versus complementary strand concentration in KCl buffer, pH 7 at 20°C with different concentrations (wt/vol) of (**a**) ethylene glycol 0% (open square), 5% (open circle) and 10% (closed triangle) and (**b**) glycerol 0% (open square), 5% (open circle) and 10% (closed triangle).

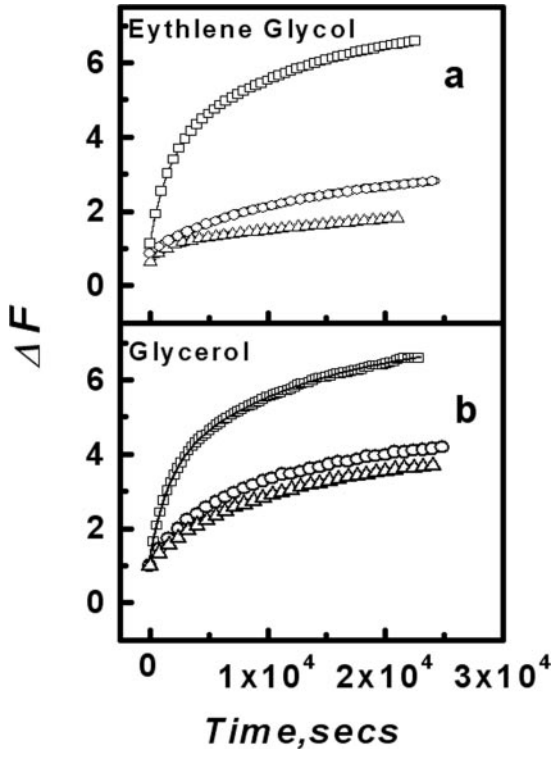


**Figure 6.** Opening up of the quadruplex-$K^+$ (30 nM) at 20°C upon addition of equimolar concentration of C-strand measured in 50 mM MES buffer, pH 7 containing 100mM KCl in the presence of different concentrations of (**a**) ethylene glycol and (**b**) glycerol. Concentrations used were 0% (open square), 5% (open circle) and 10% (open triangle). For clarity only data points of 500 s interval are plotted for each dataset and the solid lines show exponential curves described in the text, to fit the data.

where fluorescence intensity change at 520 nm was observed as a function of time. Kinetics data were analyzed as described above and the respective parameters tabulated in Table 1. The observed rate constants were 8.14 (±0.3) × $10^{-5}$ $M^{-1}$ $s^{-1}$ and 8.11 (±0.3) × $10^{-5}$ $M^{-1}$ $s^{-1}$ in the presence of 5 and 10% (wt/vol) ethylene glycol, whereas in the case of 5 and 10% (wt/vol) glycerol, the values were 7.98 (±0.2) × $10^{-5}$ $M^{-1}$ $s^{-1}$ and 7.95 (±0.1) × $10^{-5}$ $M^{-1}$ $s^{-1}$, respectively. This implies that the presence of osmolyte delays the hybridization process for duplex formation.

**Table 1.** Thermodynamic and kinetic parameters of $(G_3TTA)_3G_3$ at 20°C in different experimental conditions

| | $K_A$ ($M^{-1}$) | <Γ> (s) | $k_{obs}$ ($M^{-1}$ $s^{-1}$) | $D_{eq}$ (nM) | $Q_f$ (nM) | $D_{eq}/Q_0$ |
|---|---|---|---|---|---|---|
| Control | $3.86 \times 10^7$ | 9340 | $10.7 \times 10^{-5}$ | 12.4 | 17.6 | 0.41 |
| 5% EG | $2.4 \times 10^7$ | 12284 | $8.14 \times 10^{-5}$ | 9.8 | 20.2 | 0.33 |
| 10% EG | $1.2 \times 10^7$ | 12318 | $8.11 \times 10^{-5}$ | 6.6 | 23.4 | 0.22 |
| 5% GLY | $2.6 \times 10^7$ | 12518 | $7.98 \times 10^{-5}$ | 10.2 | 19.8 | 0.34 |
| 10% GLY | $1.3 \times 10^7$ | 12563 | $7.95 \times 10^{-5}$ | 6.9 | 23.1 | 0.23 |
| 1:5 (G:TMPyP4) | $2.7 \times 10^7$ | 12987 | $7.7 \times 10^{-5}$ | 10.4 | 19.6 | 0.35 |

$K_A$ is the equilibrium constant for telomeric duplex formation. <Γ> is the mean time constant. $k_{obs}$ is the observed rate constant. $D_{eq}$, $Q_f$ and $D_{eq}/Q_0$ are duplex, free quadruplex concentrations and fraction of duplex at equilibrium when equimolar concentration of quadruplex and complementary strand (30 nM) are mixed together in 50 mM MES buffer, pH 7 with 100 mM KCl.

## Role of G-Quadruplex interacting molecules on the transition

Hurley's group provided (32,33) the first direct evidence that *c-myc* expression is controlled by a quadruplex-to-duplex transformation. They showed that the duplex DNA could be effectively converted to G-quadruplex DNA in the presence of a small ligand cationic porphyrin (TMPyP4). Here, we have examined the role of such G-quadruplex interactive drug on quadruplex to duplex transition. The study involved the evaluation of relative stability of quadruplex (30 nM) in the presence of quadruplex selective drug, TMPyP4 (150 nM). We observed that the presence of TMPyP4 led to a significant quenching of TAMRA fluorescence, but had a moderate effect on fluorescein intensity. The plot of fluorescence intensity at 520 nm versus temperature displayed a sigmoid curve that exhibited a $T_m$ of 77.7 (±0.5)°C (Supplementary Figure S4). This finding implies that presence of the drug favors quadruplex formation, as the observed $T_m$ was 17.2°C higher than that in the absence of ligand. Next, we determined the binding affinity of the quadruplex (12 nM) to its respective complementary strand in the presence of 60 and 120 nM TMPyP4 (1:5 and 1:10 quadruplex to porphyrin ratio). Analysis of

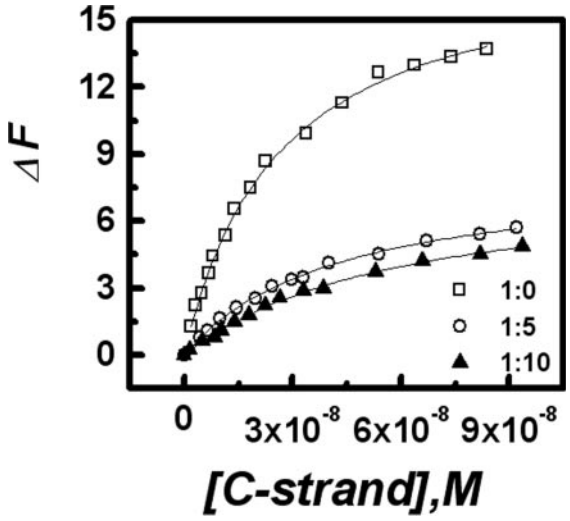


**Figure 7.** Plots of relative fluorescence emission intensity of Quadruplex-$K^+$ (12 nM) ($\Delta F$ as described in the text) versus complementary strand concentration in KCl buffer at 20°C with different concentrations of TMPyP4, 0 nM (open square), 60 nM (open circle) and 120 nM (closed triangle).

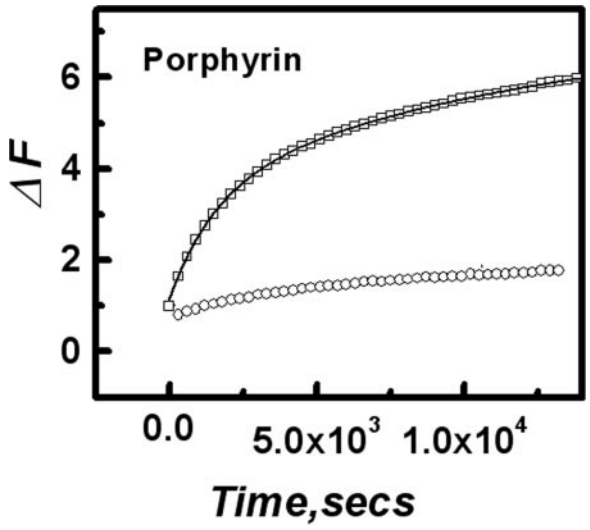


**Figure 8.** Opening up of the quadruplex-$K^+$ (30 nM) at 20°C upon addition of equimolar C-strand measured in 50 mM MES buffer with 100 mM KCl, pH 7 in the absence and presence of 150 nM of TMPyP4. Plot showing 0 nM (open square), 150 nM (open circle) of TMPyP4.

the data indicates that increase in the concentration of TMPyP4 decreases the binding affinity of the quadruplex toward its complementary strand (Figure 7). In the absence of ligand, the affinity at 20°C was estimated to be 3.86 (±0.20) × $10^7$ $M^{-1}$, whereas the binding affinities estimated in the presence of 60 and 120 nM TMPyP4 were 2.7 (±0.3) × $10^7$ $M^{-1}$ and 1.5 (±0.2) × $10^7$ $M^{-1}$, respectively. Subsequently, the kinetics of quadruplex (30 nM) opening was followed in the presence 150 nM TMPyP4 (Figure 8). The kinetic data was analyzed as described above, and the respective parameters presented in Table 1. The observed rate constant was found to be 7.7 (±0.32) × $10^{-5}$ $M^{-1}$ $s^{-1}$ at 1:5 quadruplex to porphyrin ratio.

## DISCUSSION

In the genomic context, multi-stranded DNA secondary structures formation in the region other than the end of a chromosome, are in competition with the normal WC duplex structures that is formed by the interaction with the complementary strands. However, as the genetic information encoded by DNA must be passed on to the next generation, a mechanism for interconversion between these multi-stranded secondary structures and WC duplex structures must be available. Using the human telomeric repeat, $d(G_3TTA)_3G_3$ as a model sequence, we have here examined the Quadruplex–WC duplex equilibrium under osmotic stress and in the presence of quadruplex selective binding ligand. We chose a fluorescence based study to work at reasonably low concentration, which could not have been possible with UV or CD, and carried out extensive FRET analysis to use it as a tool to verify the structure formation, stability of quadruplex, and to follow the quadruplex to duplex transition under different environmental settings. Recently, we reported successful employment of FRET in following the quadruplex to WC duplex transition of the thrombin binding aptamer (23). Our study showed that intramolecularly folded secondary structures formed by G-rich strand are kinetically trapped species and may occur under specialized conditions (such as replication, recombination, transcription and telomeric DNA elongation), which favors the formation of these secondary structures over WC duplex formation. In the current study, we have mimicked such specialized conditions and traced the opening of dual labeled 21mer d(GGG TTA GGG TTA GGG TTA GGG).

CD spectra (Supplementary Figure S1) of this 21mer human telomeric DNA in 100 mM KCl, 50 mM MES buffer, pH 7 showed a positive band at 292 nm and a negative band near 266 nm, which confirms that the given sequence formed an antiparallel G-quadruplex. The addition of equimolar concentration of complementary strand d(CCC TAA CCC TAA CCC TAA CCC) to the preformed quadruplex led to a shift of the positive and negative peak toward 280 and 252 nm, respectively, which corresponds to the signature signal of a duplex. However, the presence of a shoulder band near 285 nm suggests that certain fraction of quadruplex still exists in the solution. The presence of osmolytes fails to produce any structural changes or deformities in the CD spectra of the quadruplex, but the presence of broad shoulder upon addition of equimolar complementary strand indicates that crowding agents significantly prevent the duplex formation.

The Quadruplex–WC duplex competition and relative stability of the quadruplex under different environmental conditions was explored using FRET. The binding affinity of quadruplex to $K^+$ ions was found to be 2.5 (±0.3) × $10^7$ $M^{-2}$, which correlates well with reported values (41). Analysis of the melting profile of the dual labeled 5′-Fluorescein-d[$(G_3TTA)_3G_3$]-TAMRA-3′ gave the $T_m$ value of 60.5 (±1)°C, whereas the UV melting of unlabeled $d(G_3TTA)_3G_3$ in 100 mM KCl buffer gave a $T_m$ of 67.8 (±0.5)°C (Supplementary Figure S2). This observation is in agreement with the previous study (37), where *T*m measurements were performed for 21mer unlabeled $d(G_3TTA)_3G_3$, 5′-Fluorescein-$d(G_3TTA)_3G_3$-3′, 5′-$d(G_3TTA)_3G_3$-TAMRA-3′ and dual labeled 5′-Fluorescein-$d(G_3TTA)_3G_3$-TAMRA-3′ in 100 mM NaCl solution, pH 7. They observed that labeled

oligonucleotides (single or dual labeled) melts at lower temperature than the unlabeled oligonucleotide. Several reports which highlight the qualitative effects of environmental perturbations on Quadruplex to WC equilibrium are available, but very few of them have actually addressed the precise quantitative changes associated with these perturbations. To quantify the relative change in the binding affinity of the quadruplex to the complementary strand, we monitored FRET as a function of complementary strand concentration. The binding affinity of quadruplex to its complementary strand was found out to be 3.86 (±0.2) × $10^7$ $M^{-1}$ at 20°C in 100 mM KCl buffer. The same order of binding affinities was observed by Li *et al*. (30), where the binding constant of the two DNA strands in the presence of 100 mM $Na^+$ at pH 7.0 was 1.32 (±0.2) × $10^7$ $M^{-1}$. Recently, Zhao *et al*. (44) reported the kinetics of folding and unfolding of $(TTAGGG)_4$ in the presence of its complementary strand in 150 mM of $K^+$, $Na^+$ and $Li^+$ at 25 and 37°C by surface plasmon resonance (BIAcore) methods. The kinetic data depicted the value of equilibrium constant $K_F$ for the folding step as 9.0, and $K_A$, the equilibrium constant for the complementary strand binding to the opened state of the quadruplex as 7.8 × $10^{10}$ $M^{-1}$. So, the overall binding affinity between quadruplex and its complementary strand, ($K_F \times K_A$) was estimated to be 7.02 × $10^{11}$ $M^{-1}$. The obtained value is almost four orders of magnitude higher than the binding affinities derived from our study and Li *et al*. This discrepancy in the observation can be ascribed to the choice of technique employed for the study. The immobilization of the G-strand on a solid support used in surface plasmon resonance tends to destabilize the quadruplex structure in spite of a spacer present between the solid support and the G-strand, which may be, is responsible for the discrepancy in binding affinities between the studies described here.

Unfolding of the quadruplex in the presence of its complementary strand, to form a WC duplex, is a two-step process. Recently, measurement of the unfolding rate of fluorescently labeled human telomere repeats using similar technique (FRET) showed that the hybridization reaction of the quadruplex to the complementary C-rich strand is second order (28). This finding indicates that the rate-determining step of the process is the hybridization (second step) rather than the unfolding of the quadruplex (first step), although the reaction occurs by means of an open intermediate. In another study (27), kinetics of quadruplex opening using PNA was zero order in nature. Analysis of our kinetic data shows that opening of the quadruplex complex in the presence of its complementary strand leading to WC duplex formation follows second order kinetics, which indicates the involvement of an 'obvious' rate-determining step and the rate constant obtained was 10.7 (±0.3) × $10^{-5}$ $M^{-1}$ $s^{-1}$ at 20°C in 100 mM KCl solution. Recently, Li *et al*. (30) through stopped-flow CD kinetics observed rate constant $k_{obs}$ as 8.06 (±0.4) × $10^{-3}$ $s^{-1}$ for duplex formation by $dG_3(T_2AG_3)_3$ and its complement in 50 mM NaCl buffer which is 100 times more than the value obtained in the present study. This explains that the opening up of $K^+$-quadruplex is more difficult than that of the $Na^+$-quadruplex, leading to a lower rate constant.

Cell cytoplasm contains a large concentration of high-molecular-weight components that contribute to a substantial part of the volume of the medium. These crowding agents affect biochemical processes, such as conformational transitions and assembly of macromolecular structures, protein folding, protein aggregation etc. Molecular crowding could have a strong affect both on the equilibrium and on the rate of reactions involving macromolecules. It should be noted that properties and interaction of macromolecules in biochemical experiments *in vivo* are usually studied in dilute solutions (lower than 0.1 g/liter), where the effect of crowding is neglected. To understand the biochemical processes that occur in a living cell, crowding conditions should be simulated in experiments *in vitro*. Both low and high molecular-weight crowding agents can imitate the biochemical effects of crowding. Miyoshi *et al*. (31) have reported structural polymorphism induced by molecular crowding, but the influence of crowding agents on the equilibrium and on the rate of reactions remain unaddressed. In our study, we explored the effect of such agents on the stability of quadruplex and on the Quadruplex–WC duplex equilibrium. Crowding agents, such as ethylene glycol and glycerol, stabilize the quadruplex and bring about the reconfiguration of DNA water layers by altering the water activity. We observed a decrease in the binding affinity toward the complementary strand upon increasing the osmolytes concentration. Kinetic analysis also showed that the presence of osmolyte delays the hybridization process. The observed rate constants were 8.14 (±0.3) × $10^{-5}$ $M^{-1}$ $s^{-1}$ and 8.11 (±0.3) × $10^{-5}$ $M^{-1}$ $s^{-1}$ in the presence of 5 and 10% (wt/vol) ethylene glycol, whereas in the case of 5 and 10% (wt/vol) glycerol, the values were 7.98 (±0.2) × $10^{-5}$ $M^{-1}$ $s^{-1}$ and 7.95 (±0.1) × $10^{-5}$ $M^{-1}$ $s^{-1}$, respectively. Though the presence and absence of osmolytes produced a considerable difference in the rate constants, not much change was observed on increasing the osmolyte concentration from 5 to 10%. Analysis of the melting profile of the quadruplex in the presence and absence of osmolytes also supported the above findings, where a higher $T_m$ value in the presence of osmolytes indicated stabilization of the quadruplex structure. This increasingly stable quadruplex, thus, exhibited a lower binding affinity and consequently, slower hybridization kinetics to its respective complementary strand.

The binding of cationic porphyrin $H_2$TMPyP4 to quadruplexes formed in *c-myc* promoter region and telomeric sequences has been investigated intensively (32–35), but how these G-interactive drugs perturb the equilibrium has not been explored. We have investigated the influence of TMPyP4 on the Quadruplex–WC duplex equilibrium. This ligand not only stabilizes quadruplex but also delays the association of the two strands to form duplex. The melting profile of the quadruplex revealed a higher thermostability of the secondary structure in the presence of TMPyP4, as depicted by the rise in $T_m$. This higher stabilization of the quadruplex structure was also indicated in our binding affinity analysis that showed that the presence of TMPyP4 lowered the binding affinity of the quadruplex to its complementary strand. The estimated binding affinity of the quadruplex to its complementary strand in the absence of the ligand was found to be 3.86 (±0.2) × $10^7$ $M^{-1}$, whereas in the presence of 60 and 120 nM TMPyP4 it was reduced to 2.7 (±0.3) × $10^7$ $M^{-1}$ and 1.5 (±0.2) × $10^7$ $M^{-1}$, respectively. The rate constant obtained from the kinetic analysis upon hybridization of quadruplex to its equimolar complementary strand in the presence of five times excess of TMPyP4 was found out to be 7.7 (±0.32) × $10^{-5}$ $M^{-1}$ $s^{-1}$, which was lower than that obtained

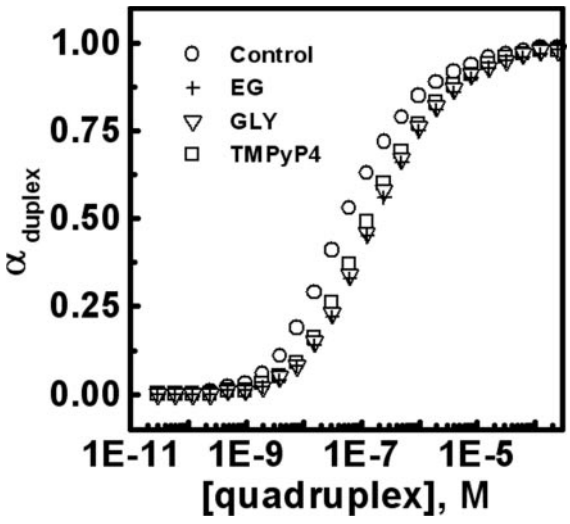


**Figure 9.** Dependence of duplex formation at equilibrium on strand concentrations in a mixture of equimolar ratio of $(G_3TTA)_3G_3$ and $C_3(TAAC_3)_3$, under different experimental conditions The amount of duplex at equilibrium, $D_{eq}$, was calculated from the binding affinity toward the complementary strand obtained from different experimental conditions, using the equation $K = D_{eq}/(Q_0 - D_{eq}) \times (C_0 - D_{eq})$, where $Q_0$ and $C_0$ ($Q_0 = C_0$) are the initial quadruplex and complementary strand concentration. Control (open circle), 10% ethylene glycol (plus sign), 10% glycerol (open triangle) and TMPyP4 (open square).

in the absence of the ligand. The presence of ligand, thus, slowed the hybridization of the quadruplex to its complementary strand. The given observation was in consensus with the above findings that indicated that the presence of the ligand TMPyP4 stabilizes quadruplex structure, thereby, favors its formation over Watson and Crick base pairing. The thermodynamic and kinetic parameters derived from such studies would promote better designing of G-quadruplex recognizing or interacting molecules and establishment of therapeutic selectivity (45).

Using equilibrium binding constants of the quadruplex to its complementary strand obtained from this study, we calculated the amount of duplexes ($D_{max}$), free quadruplexes ($Q_f$) and fraction of quadruplexes converted to duplex after attainment of equilibrium under each condition, as shown in Table 1 (Figure 9). We found that quadruplexes were the predominant species in each condition. From the experimental binding constant, we calculated the fraction of duplex formed when equimolar concentrations of the G- and C-rich strands were mixed together in 100 mM KCl in the absence and presence of 10% (wt/vol) osmolytes and 1:5 quadruplex:porphyrin concentration ratio. We observed that the formation of duplex was dependent on initial strand concentration used at 20°C. At $10^{-9}$ M or lower, $d(G_3TTA)_3G_3$ mainly exist in the quadruplex form, whereas at higher strand concentration the fraction of duplex increases and approaches to its maximum at the concentration $10^{-6}$M or higher. In 100 mM KCl solution at equilibrium, 1:1 quadruplex:duplex would exist upon the addition of 50, 130, 144 and 116 nM of equimolar mixture of both the strands in the absence and presence of 10% ethylene glycol, 10% glycerol and 150 nM TMPyP4, respectively. On the other hand, in 100 mM KCl solution, when 30 nM of each components, i.e. quadruplex and the complementary strand, are mixed together, the amount of quadruplex present in the system under equilibrium is 17.6, 23.4, 23.1 and 19.6 nM in the absence and presence of 10% ethylene glycol, 10% glycerol and 150 nM TMPyP4, respectively.

## CONCLUSIONS

The present study examines the sensitivity of Quadruplex–WC duplex equilibrium to various environmental conditions, such as osmotic stress and quadruplex selective small molecule. From extensive FRET analysis, we observed that both the quadruplex and WC duplex forms of $d(G_3TTA)_3G_3$/$d(C_3TAA)_3C_3$ are thermodynamically stable under physiological condition and coexist in equilibrium. Molecular crowding bears similarity to natural scenario, and quadruplex selective cationic porphyrin relevant in the pharmacological context, favor quadruplex formation, and hence, delays duplex formation. In summary, the equilibrium and rate of the interconversion between WC duplex and quadruplex depends on the stability of the quadruplex and its alternative duplex form, which can be modulated by the fluctuation of the $K^+/Na^+$ concentration, solute concentration and with the introduction of selective pharmacological/therapeutic perturbation inside of the cell to exploit quadruplexes as a drug target.

## SUPPLEMENTARY DATA

Supplementary Data are available at NAR Online.

## ACKNOWLEDGEMENTS

S.M. acknowledges Prof. Samir K. Brahmachari for constant support and CSIR for funding this research. N.K. acknowledges research fellowship from CSIR. The authors wish to thank 'The Centre for Genomics Applications, (TCGA)' at IGIB granted by CSIR and DST for providing instrumental facility and technical help. The authors also acknowledge the reviewers for their suggestions. The Open Access publication charges for this article were waived by Oxford University Press.

*Conflict of interest statement*. None declared.

## REFERENCES

1. Gellert,M., Lipsett,M.N. and Davies,D.R. (1962) Helix formation by guanylic acid. *Proc. Natl Acad. Sci. USA*, **48**, 2013–2018.
2. Balagurumoorthy,P. and Brahmachari,S.K. (1994) Structure and stability of human telomeric sequence. *J. Biol. Chem.*, **269**, 21858–21869.
3. Sen,D. and Gilbert,W. (1988) Formation of parallel four-stranded complexes by guanine-rich motifs in DNA and its implications for meiosis. *Nature*, **334**, 364–366.
4. Evans,T., Schon,E., Gora-Maslak,G., Patterson,J. and Efstratiatdis,A. (1984) S1-hypersensitive sites in eukaryotic promoter regions. *Nucleic Acids Res.*, **12**, 8043–8058.
5. Kilpatrick,M.W., Torri,A., Kang,D.S., Engler,J.A. and Wells,R.D. (1986) Unusual DNA structures in the adenovirus genome. *J. Biol. Chem.*, **261**, 11350–11354.
6. Fry,M. and Loeb,L.A. (1994) The fragile X syndrome d(CGG)n nucleotide repeats form a stable tetrahelical structure. *Proc. Natl Acad. Sci. USA*, **91**, 4950–4954.
7. Erlitzki,R. and Fry,M. (1997) Sequence-specific binding protein of single-stranded and unimolecular quadruplex telomeric DNA from rat hepatocytes. *J. Biol. Chem.*, **272**, 15881–15890.

8. Giraldo,R., Suzuki,M., Chapman,L. and Rhodes,D. (1994) Promotion of parallel DNA quadruplexes by a yeast telomere binding protein: a circular dichroism study. *Proc. Natl Acad. Sci. USA*, **91**, 7658–7662.
9. Fang,G. and Cech,T.R. (1993) The beta subunit of Oxytricha telomere-binding protein promotes G-quartet formation by telomeric DNA. *Cell*, **74**, 875–885.
10. Patel,S.D., Isalan,M., Gavory,G., Ladame,S., Choo,Y. and Balasubramanian,S. (2004) Inhibition of human telomerase activity by an engineered zinc finger protein that binds G-quadruplex. *Biochemistry*, **43**, 13452–13458.
11. Sarig,G., Weisman-Shomer,P., Erlitzki,R. and Fry,M. (1997) Purification and characterization of qTBP42, a new single stranded and quadruplex telomeric DNA binding protein from rat hepatocytes. *J. Biol. Chem.*, **272**, 4474–4482.
12. Dempsey,L.A., Sun,H., HanakahiL,A. and Maizels,N. (1999) G4 DNA binding by LR1 and its subunits, nucleolin and hnRNP D, A role for G-G pairing in immunoglobulin switch recombination. *J. Biol. Chem.*, **274**, 1066–1071.
13. Fang,G. and Cech,T.R. (1993) Characterization of a G-quartet formation reaction promoted by the beta-subunit of the Oxytricha telomere-binding protein. *Biochemistry*, **32**, 11646–11657.
14. Hurley,L.H., Wheelhouse,R.T., Sun,D., Kerwin,S.M., Salazar,M., Fedoroff,O.Y., Han,F.X., Han,H., Izbicka,E. and Von Hoff,D.D. (2000) G-quadruplexes as targets for drug design. *Pharmacol. Ther.*, **85**, 141–158.
15. Han,H.Y. and Hurley,L.H. (2000) G-quadruplex DNA: a potential target for anti-cancer drug design. *Trends Pharmacol. Sci.*, **21**, 136–142.
16. Huppert,J.L. and Balasubramanian,S. (2005) Prevalence of Quadruplexes in the human genome. *Nucleic Acids Res.*, **33**, 2908–2916.
17. Todd,A.K., Johnston,M. and Neidle,S. (2005) Highly prevalent putative quadruplex sequence motifs in human DNA. *Nucleic Acids Res.*, **33**, 2901–2907.
18. Rankin,S., Reszka,A.P., Hupper,J., Parkinson,G.N., Todd,A.K., Ladame,S., Balasubramanian,S. and Neidle,S. (2005) Putative DNA quadruplex formation within the human c-kit oncogene. *J. Am. Chem. Soc.*, **127**, 10584–10589.
19. Hardin,C.C., Watson,T., Corregan,M. and Bailey,C. (1992) Cation dependent transition between the quadruplex and Watson–Crick hairpin forms of d(CGCG$_3$GCG). *Biochemistry*, **31**, 833–841.
20. Miura,T. and Thomas,G.J. (1994) Structural polymorphism of telomere DNA: Interquadruplex and Duplex–Quadruplex conversions probed by Raman spectroscopy. *Biochemistry*, **33**, 7848–7856.
21. Deng,H. and Braunlin,W.H. (1995) Duplex to quadruplex equilibrium of the self-complementary oligonucleotide d(GGGGCCCC). *Biopolymers*, **35**, 677–681.
22. Halder,K., Mathur,V., Chugh,D., Verma,A. and Chowdhury,S. (2005) Quadruplex–duplex competition in the nuclease hypersensitive element of human c-myc promoter: C to T mutation in C-rich strand enhances duplex association. *Biochem. Biophys. Res. Commun.*, **327**, 49–56.
23. Kumar,N. and Maiti,S. (2004) Quadruplex to Watson–Crick duplex transition of the thrombin binding aptamer: a fluorescence resonance energy transfer study. *Biochem. Biophys. Res. Commun.*, **319**, 759–767.
24. Datta,B. and Armitage,B.A. (2001) Hybridization of PNA to structured DNA targets: quadruplex invasion and the overhang effect. *J. Am. Chem. Soc.*, **123**, 9612–9619.
25. Phan,A.T. and Mergny,J.L. (2002) Human telomeric DNA: G-quadruplex, i-motif and Watson–Crick double helix. *Nucleic Acids Res.*, **30**, 4618–4625.
26. Li,W., Wu,P., Ohmichia,T. and Sugimotoa,N. (2002) Characterization and thermodynamic properties of quadruplex/duplex competition. *FEBS Lett.*, **526**, 77–81.
27. Green,J.J., Ying,L., Klenerman,D. and Balasubramanian,S. (2003) Kinetics of unfolding the human telomeric DNA quadruplex using a PNA trap. *J. Am. Chem. Soc.*, **125**, 3763–3767.
28. Ying,L., Green,J.J., Li,H., Klenerman,D. and Balasubramanian,S. (2003) Studies on the structure and dynamics of the human telomeric G quadruplex by single-molecule Fluorescence resonance energy transfer. *Proc. Natl Acad. Sci. USA*, **100**, 14629–14634.
29. Risitano,A. and Fox,K.R. (2003) Stability of intramolecular DNA quadruplexes: comparison with DNA duplexes. *Biochemistry*, **42**, 6507–6513.
30. Li,W., Miyoshi,D., Nakano,S. and Sugimoto,N. (2003) Structural Competition involving G-quadruplex DNA and its Complement. *Biochemistry*, **42**, 11736–11744.
31. Miyoshi,D., Matsumura,S., Nakano,S. and Sugimoto,N. (2004) Duplex Dissociation of Telomere DNAs Induced by Molecular Crowding. *J. Am. Chem. Soc.*, **126**, 165–169.
32. Rangan,A., Fedoroff,O.Y. and Hurley,L.H. (2001) Induction of Duplex to G-quadruplex transition in the c-myc promoter region by a small molecule. *J. Biol. Chem.*, **276**, 4640–4646.
33. Jain,A.S., Grand,C.L., Bearss,D.J. and Hurley,L.H. (2002) Direct evidence for a G-quadruplex in a promoter region and its targeting with a small molecule to repress c-MYC transcription. *Proc. Natl Acad. Sci. USA.*, **99**, 11593–11598.
34. Anantha,N.V., Azam,N. and Sheardy,R.D. (1998) Porphyrin binding to Quadruplexed $T_4G_4$. *Biochemistry*, **37**, 2709–2714.
35. Haq,I., Trent,J.O., Chowdhury,B.Z. and Jentkins,T.C. (1999) Intercalative G-tetraplex stabilization of telomeric DNA by cationic porphyrin. *J. Am. Chem. Soc.*, **121**, 1768–1779.
36. Mergny,J.L. (1999) Fluorescence energy transfer as a probe for tetraplex formation: the i-motif. *Biochemistry*, **38**, 1573–1581.
37. Mergny,J.L. and Maurizot,J.C. (2001) Fluorescence resonance energy transfer as a probe for G-quartet formation by a telomeric repeat. *Chembiochem*, **2**, 124–132.
38. Simonsson,T. and Sjoback,R. (1999) DNA tetraplex formation studied with Fluorescence resonance energy transfer. *J. Biol. Chem.*, **274**, 17379–17383.
39. Cantor,C.R., Warshaw,M.M. and Shapiro,H. (1970) Oligonucleotide interactions, Circular dichroism studies of the conformation of deoxyoligonucleotides. *Biopolymers*, **9**, 1059–1077.
40. Marky,L.A. and Breslauer,K.J. (1987) Calculating thermodynamic data for transitions of any molecularity from equilibrium melting curves. *Biopolymers*, **26**, 1601–1620.
41. Ueyma,H., Takagi,M. and Takenda,S. (2002) A novel potassium sensing in aqueous media with a synthetic oligonucleotide derivative Fluorescence resonance energy transfer associated with guanine quartet-potassium ion complex formation. *J. Am. Chem. Soc.*, **124**, 14286–14287.
42. Bonnet,G., Tyagi,S., Libchaber,A. and Kramer,F.R. (1999) Thermodynamic basis of the enhanced specificity of structured DNA probes. *Proc. Natl Acad. Sci. USA.*, **96**, 6171–6176.
43. Minton,A.P. (2001) The Influence of Macromolecular Crowding and Macromolecular Confinement on Biochemical Reactions in Physiological Media. *J. Biol. Chem.*, **276**, 10577–10580.
44. Zhao,Y., Kan,Z., Zeng,Z., Hao,Y.H., Chen,H. and Tan,Z. (2004) Determining the folding and unfolding rate constants of nucleic acids by biosensor. Application to telomere G-Quadruplex. *J. Am. Chem. Soc.*, **126**, 13255–13264.
45. Mergny,J.L., Riou,J.F., Maillet,P., Teulade-Fichou,M.P. and Gilson,E. (2002) Natural and pharmacological regulation of telomerase. *Nucleic Acids Res.*, **30**, 839–865.